



Contents lists available at ScienceDirect

Optics Communications

journal homepage: www.elsevier.com/locate/optcom

Scintillation of laser beams carrying orbital angular momentum propagating in a near-maritime environment

Joe Wiedemann^{a,*}, Charles Nelson^b, Svetlana Avramov-Zamurovic^c

^a Physics Department, US Naval Academy, 105 Maryland Avenue, Annapolis, MD 21402, USA

^b Electrical and Computer Engineering Department, US Naval Academy, 105 Maryland Avenue, Annapolis, MD 21402, USA

^c Weapons and Systems Engineering Department, US Naval Academy, 105 Maryland Avenue, Annapolis, MD 21402, USA

ARTICLE INFO

Keywords:

Orbital angular momentum

OAM

Laser propagation

Near-maritime environment

Scintillation

ABSTRACT

Laser beams carrying orbital angular momentum (OAM) were propagated in a near-maritime environment along an 890 meter link across the Severn River at the United States Naval Academy. The OAM beams were generated using green light ($\lambda = 532$ nm) and etched spiral phase plates with different topological charges. The light intensity fluctuations of Gaussian and beams carrying OAM with topological charges of 1, 6, and 8 were measured and the scintillation indices of each beam were compared. Additionally, atmospheric turbulence was measured using a co-aligned scintillometer along the 890 meter propagation path. During testing, a wide range of atmospheric conditions occurred and the refractive index structure parameter measurements ranged from 5×10^{-14} down to $5 \times 10^{-15} \text{ m}^{-2/3}$. Our measurements of transmitted voltage in the radial intensity across the maritime link, and calculated scintillation index, for the Gaussian beam and laser beams carrying OAM indicate a weak reduction in scintillation index for increasing topological charge. To reduce the measurement uncertainty and improve upon statistical significance of our findings, additional testing is needed.

1. Introduction

Understanding and mitigating the interaction between laser light and random media, such as atmospheric turbulence, is a fundamental challenge in optical communications [1,2]. As both military and civilian sectors have increased their pursuit of advancement in the area of free space optical communications much of the research effort has been focused on the mitigation of turbulence and scintillation effects through the use of source partial coherence [3–5], aperture averaging [6], sparse aperture detectors [7,8], wavelength diversity [9], source temporal variations [10], polarization diversity [11–14] and more recently, non-uniformly correlated partially coherent beams [15–17] as well as the potentially promising use of optical orbital angular momentum [18]. Orbital angular momentum in particular has application in communications [19,20] for minimizing cross-talk across channels [7] and use of the orthogonality of the OAM modes to increase bandwidth to the terabit range [19]. While these studies are principally motivated by the wide bandwidth capabilities and tactical advantages of free space optical communication, there remain challenges with regards to understanding light fluctuations and specifically with regards to light fluctuations in beams carrying OAM through real atmospheric turbulence.

Random atmospheric turbulence distorts free space propagation as the stochastic changes in the index of refraction of the atmosphere

deteriorates laser beams. Our experiments were carried out to test the scintillation performance of the beams with topological charges 1, 6 and 8 as compared to the propagation of a Gaussian beam in a near-maritime environment. A Scintec © BLS450 Large Aperture scintillometer was co-aligned to measure the strength of atmospheric turbulence. While our findings were not conclusive as to a clear, statistically significant, scintillation improvement on optical propagation of beams carrying OAM as compared to Gaussian beams, the possibility of a weak trend was deemed viable and additional experimentation is required to confirm it. To the best of our knowledge, this paper is the first to report experimental results of optical beams carrying OAM propagating nearly a kilometer over the water in a near-maritime environment.

The paper is organized as follows: the methods and experimental design and set-up is discussed in Section 2, followed by data analysis and results in Section 3. Lastly Section 4 concludes this paper.

2. Methods and experimental design

A Gaussian laser beam can be converted to a beam carrying OAM by using a spiral phase plate or a spatial light modulator [22]. In both cases, there is an index of refraction spatial gradient that creates the helical phase front with a characteristic annular intensity and null,

* Corresponding author.

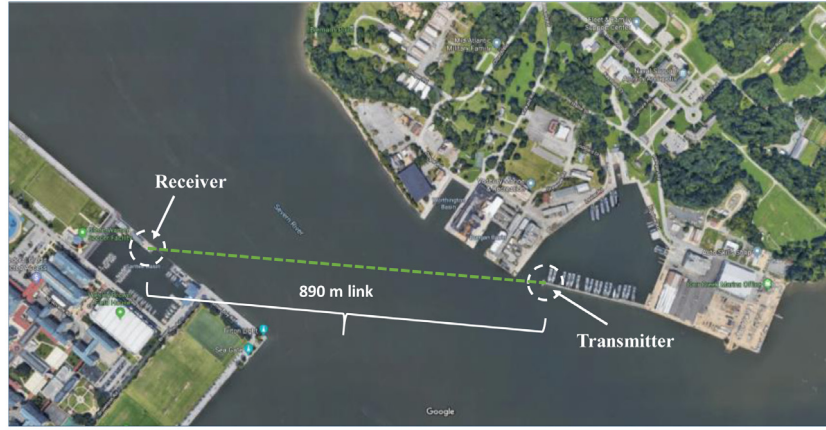
E-mail address: m217128@usna.edu (J. Wiedemann).

<https://doi.org/10.1016/j.optcom.2019.124836>

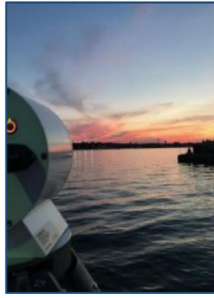
Received 4 September 2019; Received in revised form 24 October 2019; Accepted 27 October 2019

Available online xxxx

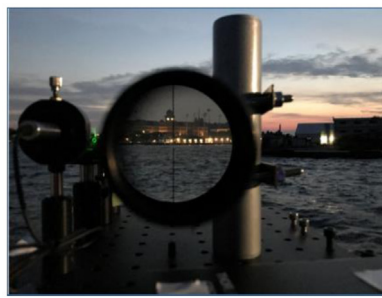
0030-4018/Published by Elsevier B.V.



a)



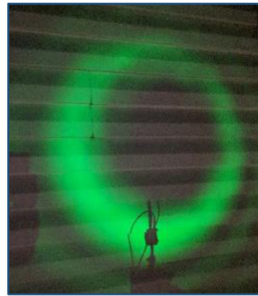
b)



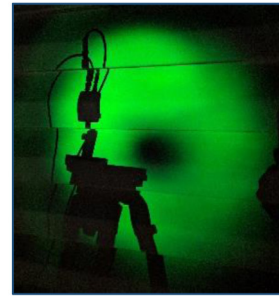
c)



d)



e)



f)

Fig. 1. Experimental set up: (a) 890 m laser and scintillometer links at the US Naval Academy [21], (b) scintillometer transmitter (c) laser diode system set up, (d) scintillometer receiver (e) beam carrying OAM with topological charge 6 (540 m link) and (f) beam carrying OAM with topological charge 1 (540 m link).

vortex, along the central propagation axis. Each phase plate is unique to both topological charge and the wavelength of the light, as the wavelength determines the values for the minimum and maximum index of refraction. With regards to the glass phase plate, the topological charge is the number of cycles the index of refraction increases from the minimum to the maximum in the 2π radian cycle.

Our primary motivation in this research is to explore the radial intensity fluctuations, or scintillations, of a beam carrying OAM in comparison to a Gaussian beam when propagating in near-maritime atmosphere. We focus on radial intensity fluctuations, for applications in optical communications. One measure of turbulence strength is quantified with the refractive index structure constant, C_n^2 . The effect of the turbulence on the laser beam is quantified with the scintillation index (SI). Assuming that the light intensity is measured at a selected point in the radial portion of the beam over time, thus creating a data set $\{I_n\}$ where n is the number of measurements, scintillation index

relates the measured intensity average $\langle I \rangle$ and its variance $\langle I^2 \rangle$:

$$SI = \frac{\langle I^2 \rangle}{\langle I \rangle^2} - 1 \quad (1)$$

2.1. Experimental set up

A 532 nm laser diode that was modulated with etched spiral phase plates and a photodetector were used to establish an 890 m optical link in a near-maritime environment across the Severn River at the US Naval Academy grounds (see Fig. 1a). Additionally, a co-aligned, commercial scintillometer was used to measure the optical turbulence every minute, in the form of C_n^2 along the propagation path.

An optical scope was used to align and direct the laser over the 890 m link. 90° phase plate flip mounts secured the 3 phase plates of topological charges 1, 6, and 8, and could be easily rotated into and out of the laser beam path (see Fig. 2).

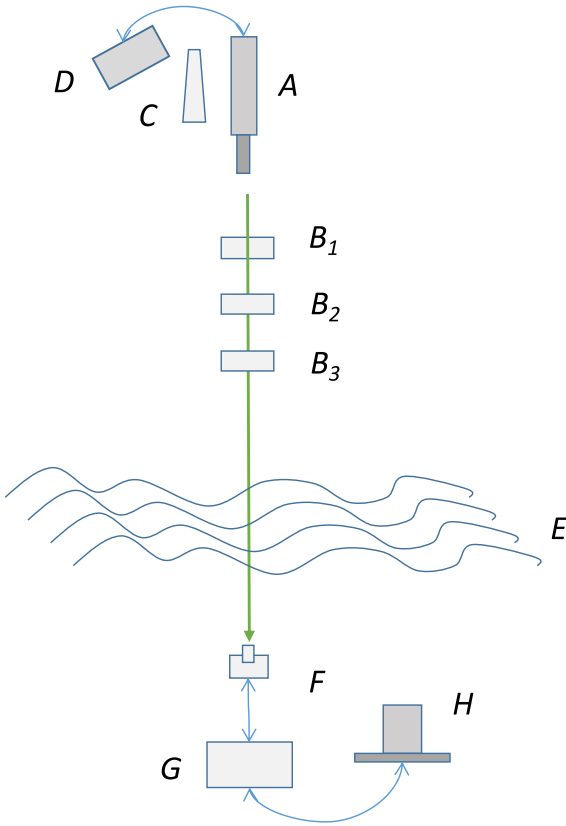


Fig. 2. Experimental equipment schematic, A—532 nm laser diode source, B_1 —topological charge 1 plate with flip mount, B_2 —topological charge 6 plate with flip mount, B_3 —topological charge 8 plate with flip mount, C—optical scope, D—power supply, E—atmospheric channel, F—photodetector, G—DAQ, H—computer.

An amplified photodetector with a surface area of 100 mm², a 532 nm wavelength filter to eliminate background light, and a 2.54 cm plano-convex lens was used to maximize power. The detector was set on an optical rail with an adjustable post for lateral and vertical fine adjustments and a DAQ was used to record optical intensity data at 10 kHz. Data was collected at the point of maximum power for each laser beam. Minor adjustments of the photodetector laterally, vertically, and in rotation allowed us to locate the point of maximum power in the experimental beam. This point was in the annulus of the vortex beams and the center of the Gaussian beam. Data was recorded for approximately 1 min per trial with the sampling rate of 10 kHz.

A preliminary outdoor experiment was conducted on March 29, 2019 at 540 m across the Severn River. While we were able to collect optical propagation data, the path was not co-aligned with the scintillometer making it hard for reliable comparisons with the atmospheric turbulence. Subsequently, we established and collected data over an 890 m link on May 18 and 19, 2019. The laser diode transmitter was positioned at the Naval Station (on the right side, see Fig. 1a) and the receiver was located at the Santee Basin (on the left side) at the United States Naval Academy. We established a link for all three charges and the Gaussian beam and recorded seven runs of each scenario, alternating through the four beams in steady procession. The measurements were coupled with the scintillometer data in order to establish the optical turbulence associated with each data collection run.

3. Data analysis and results

Our experimentation captured over 14.8 million data points over 28 experimental runs in a broad swath of atmospheric turbulence in a

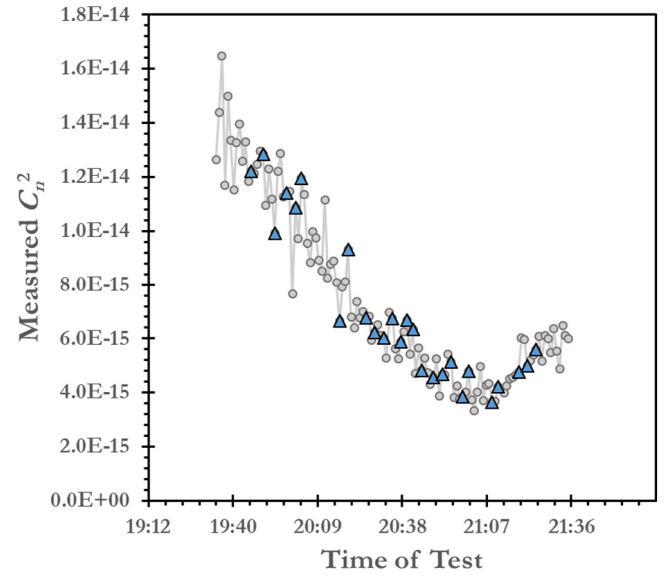


Fig. 3. Scintillometer measurements C_n^2 for 890 m link. Measurements (gray circle), and measurements that coincide with an OAM beam (blue triangle).

real near-maritime environment. This has been a unique opportunity to capture such extensive data about the performance of a laser beam carrying OAM in order to characterize the beams.

Fig. 3 displays all scintillometer measurements during our 890 m test with circles. Experimental data points where we collected data on beams carrying OAM are marked with triangles. The atmospheric turbulence fluctuated markedly during the testing which complicated the analysis, and which provided an excellent opportunity to gain greater insight into how beams carrying OAM propagate in a real maritime environment. To assure reliability of data captured in this real environment, over 600,000 data points were collected for each of the topological charges as they were tested in the same sequential order over the course of the field experiment.

In Fig. 4, the C_n^2 data and scintillation index measurements for the corresponding charges are given. Note the correlation between changes in C_n^2 with measured scintillation index regardless of charge. Mapping the SI and C_n^2 simultaneously allows us to see the broad trend of the interaction between laser beams and the turbulent medium. The sudden jumps in SI generally correlating to spikes in the measured C_n^2 is an important relationship. Furthermore, Fig. 4 demonstrates how one of the challenges in optical communications is the variation in signal degradation in relation to the changing turbulence. Fig. 4 should not be taken to imply that certain charges, such as topological charge 1, are more sensitive to turbulence as it has a sudden spike. If there was a strong difference in the SI performance for the different topological charges, we would expect the trend lines to have a consistent vertical separation. However, the trend lines for all four tested topological charges are tightly grouped and there is no consistent separation between them. Thus, we can see that the fluctuations of index of refraction, as measured by C_n^2 , are far more significant than the topological charge in determining SI .

3.1. Average scintillation index analysis

Mean scintillation index for all seven trials is given in Table 1. Standard deviation across seven data sets is consistent. Percent decrease of SI is calculated per Eq. (2), where n is an index that is placeholder for each of the topological charges:

$$\%SI \text{ Reduction} = \frac{Avg_{gaussian} - Avg_n}{Avg_{gaussian}} \times 100 \quad (2)$$

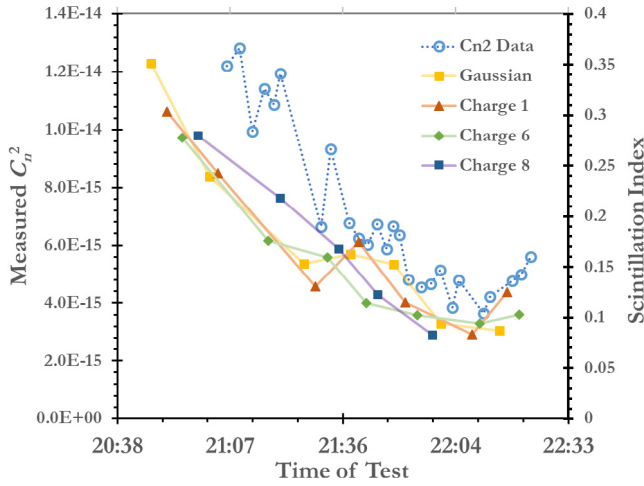


Fig. 4. Scintillation Index, C_n^2 correlation. The C_n^2 data (open circles and dashed line) trend is correlated with SI of the laser beams (solid markers and lines).

Table 1

Average SI as a function of topological charge for the complete set of data.

Topological charge	Average SI	SI Standard deviation	% SI reduction
0	0.1773	0.09186	–
1	0.1678	0.07875	5.35
6	0.1466	0.06559	17.31
8	0.1493	0.07653	15.79

Table 2

Two sample T-test of SI measurements for laser beams carrying OAM in comparison to a Gaussian beam.

	Gaussian beam	Topological charge 1	Topological charge 6	Topological charge 8
T test p-values	–	0.840	0.488	0.549

There is a noticeable grouping between the Gaussian (charge 0) and charge 1 that lies slightly higher than the charge 6 and 8 grouping. This is suggestive of a possible decrease in SI for higher topological charges, however the possible decrease is inconclusive due to the relative value of the standard deviation. As evident in Table 1, the reduction in SI is less than the value of the standard deviation. The standard deviation for SI is approximately half of the average SI value for each charge, which creates far too much overlap between the SI ranges for the charges to conclusively determine a trend.

Potential reduction of SI with increase of topological charge was studied by the two-sample T-Test. The mean values for each charge were compared against the mean for the Gaussian beam to determine if the decrease we see is statistically significant. Table 2 demonstrates that each comparison between the laser beam carrying OAM and the Gaussian beam is subject to significant statistical uncertainty. As seen with topological charge 1, the p-value is so close to 1 that we did not establish certainty that the topological charge 1 beam was different than the Gaussian beam beyond statistical variation. The test does not compare the SI , but demonstrates how likely it is that the average SI for that topological charge could have been found in the Gaussian beam data.

When the SI of beams with different topological charges are compared to the Gaussian data our results do not rule out the possibility of slight improvement, as shown in Fig. 5. Additional experimental runs could potentially reduce the statistical variation.

Fig. 5 displays the average SI for topological charges 0, 1, 6, and 8 for the entire experimental data set, for all 28 experimental runs that includes 14.8 million data points. Each data point is the average

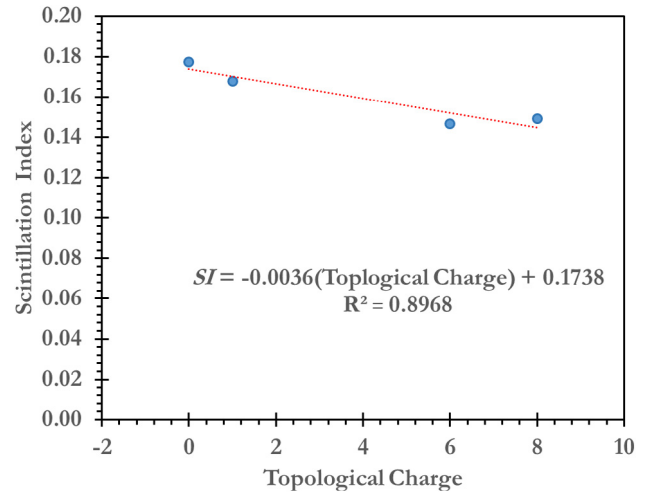


Fig. 5. Plot of SI as a function of all tested topological charges with a linear regression.

from the complete set of SI for its respective charge. The trend line is calculated using a linear fit and the slope of -0.0036 shows a weak reduction in SI for increasing topological charge. The R^2 value confirms the high probability that this weak trend exists, but the t-test outlined above challenges the certainty. Nonetheless, the groupings between the Gaussian beam and topological charge 1 in comparison to the topological charges 6 and 8 graphically reinforce the potential existence of different performance based on topological charge. Significantly higher topological charges could be tested to gain a more accurate conception of trend behavior.

3.2. Dependence of the data on measured C_n^2

In order to explore mitigating the effects of changing C_n^2 , we compared the ratio of the SI to the C_n^2 (with the order of magnitude adjusted from 10^{-18} to 10^{-2} exclusively for easier bookkeeping). The ratio was defined via Eq. (3):

$$\text{Avg. } SI / C_n^2 \text{ Ratio} = \frac{C_n^2}{SI} \times 10^{16} \quad (3)$$

The average power for C_n^2 is $10^{-15} \text{ m}^{-2/3}$, and the SI is generally around 10^{-3} , so this ratio results in a value on the order of 10^{-18} . Since the results are all the same order of magnitude, the leading zeros do not change the trend and are unnecessary.

Fig. 5 shows how during the test, the C_n^2 dropped markedly through the early testing and then leveled out to an extent. The linear ratio between scintillation index and C_n^2 comes from the Rytov turbulence model, where within a constant, the variation of a plane wave and C_n^2 are linearly proportional [1]. Under the assumption of a plane wave, which we assumed to be reasonable for our experimental set up, given the scale of the photodetector in comparison to the laser beam, the scintillation can be given by the Rytov variance, as seen in Eq. (4):

$$\sigma_R^2 = 1.23 C_n^2 k^{7/6} L^{11/6}, \quad (4)$$

where σ_R^2 the Rytov variance, k is the wavenumber, and L is the propagation path length [1]. Thus, for the same wavelength of light over the same path, the Rytov variance and C_n^2 are linearly proportional.

Table 3 compares the different topological charges by the average ratio of their scintillation index to the C_n^2 value for the particular run. The ratio established, potentially reduced the standard deviation from approximately 50% of the principle value to just over 10%, as highlighted in Table 3. Relative to the reduction of SI for increasing topological charge by comparing the average SI for each charge, a very

Table 3
Average ratio value for tested laser beams.

Charge	Average SI/C_n^2 ratio	Standard dev	% SI reduction
0	0.2477	0.0535	–
1	0.2355	0.0233	4.92
6	0.2309	0.0385	6.78
8	0.2238	0.0310	9.65

Table 4
Two sample t-test for the ratio of the SI to C_n^2 .

	Gaussian beam	Topological charge 1	Topological charge 6	Topological charge 8
T test p-value	–	0.594	0.514	0.332

similar weak reduction in SI for increasing topological charge was seen by comparing the ratio of the SI to C_n^2 for each charge. The ratio draws out the relationship between SI and C_n^2 for each charge. Each charge should have a consistent ratio of how much the laser beam degrades to the atmospheric turbulence, and improved performance becomes clear when this ratio decreases. In Table 3, the average value of this ratio for each charge is shown along with the standard deviation for ratio values in the set of trials. The % SI reduction displays how much each topological charge decreased the ratio in comparison to the Gaussian beam.

Of note, the same trend of a slight reduction for higher topological charges is observed and there was a slight improvement in the p-values of the two sample T-test. Not clearly statistically significant, but this provides better evidence that this trend potentially exists and that more testing should be done. In Table 4 the value of the ratio for each charge for each trial is listed, and the p-value from the two sample t-test is emphasized at the bottom.

The two sample T-test on ratio data compares the mean value of the ratio to the complete set of the charges against the mean value of the ratio for the Gaussian beam trials. The p-values for the ratio suggest a more conclusive result than the p-values comparing only the SI , because the ratio inherently takes into account the different C_n^2 values and the variance is going to reflect the variance of both the SI and the C_n^2 . These p-values are neither decisive nor indecisive, but they are suggestive of a weakly decreasing trend.

The changing turbulence created a comprehensive testing environment to study the properties of beams carrying OAM in a real near-maritime environment, but the variation in the turbulence made it more difficult to distill the specific behavior of the laser beam in face of the multi-faceted influences. As seen in Figs. 3 and 4 there is variance in the turbulence between the experimental test-runs which could account for the lack of strong statistically significant trend. However, the weak trend could still exist as discussed in Section 3. In Fig. 6 we show that this extensive turbulence profile potentially contributed to variation in the measured voltage for the same beam, which may be linked to the uncertainty in our weak trend. More significant than the C_n^2 measurements is the lateral separation that is evident within each topological charge. This is another issue that could be resolved by additional testing is needed.

4. Conclusion

We established an 890 m link across the Severn river for a Gaussian laser beam along with laser beams carrying OAM with 3 different topological charges 1, 6, and 8 in order to create a novel test to explore the behavior of these beams in a near maritime environment. As expected with testing in an open field environment, the experimentation condition variations were a significant challenge in obtaining data sets that were acceptable for the analysis. However, these variations also serve as a more comprehensive lens into the behavior of laser beams

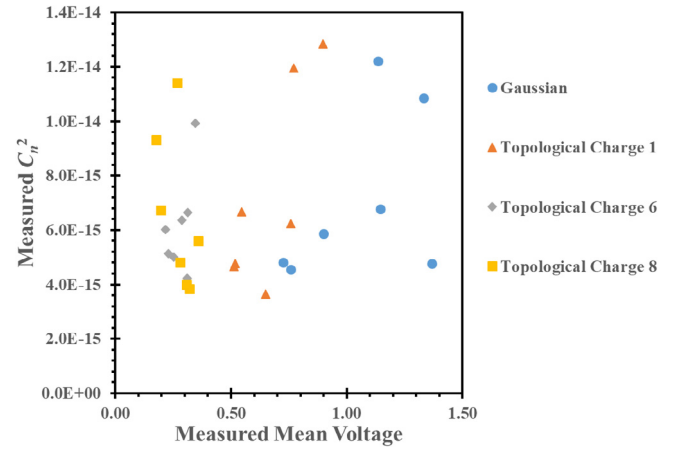


Fig. 6. C_n^2 as a function of mean voltage measured using the photodetector.

carrying OAM in a near maritime environment. The weak decrease in scintillation index for increasing topological charge still carries statistical uncertainty. Nonetheless, as our analysis has shown through comparison of the measured scintillation index and ratio of scintillation index to C_n^2 , there is a noticeable possibility that the trend exists. Our outdoor experiment is an important bridge in the exploration of laser beams carrying OAM that warrants testing beyond laboratory experiments and simulations into further testing in real turbulence. Relevant literature has found that there is a reduction in SI in the vortex [23] of the laser beam carrying OAM for higher topological charges, and it is encouraging that our experimentation could suggest a similar trend for the radial beam intensity, which is actually used to transmit data. Future testing could consider the use of a beam splitter to simultaneously propagate a Gaussian beam with a beam carrying OAM in order to subject the two beams to nearly the same levels of optical turbulence, and ensuring capturing a uniform intensity at the detector point for various scenarios tested.

Acknowledgments

We would like to acknowledge the generous support by the Office of Naval Research, USA, Midshipman Jon Copley for assistance in experimental set-up and data collection, and NAVAIR for providing the spiral phase plates.

References

- [1] L.C. Andrews, R.L. Phillips, *Laser Beam Propagation Through Random Media*, second ed., SPIE Press, Bellingham, WA, 2005.
- [2] A. Ishimaru, *Wave Propagation and Scattering in Random Media*, Vols. 1 and 2, Academic, San Diego, Calif., 1978.
- [3] F. Wang, X. Liu, Y. Cai, Propagation of partially coherent beam in turbulent atmosphere: a review (invited review), *Prog. Electromagn. Res.* 150 (2015) 123–143.
- [4] V.A. Banakh, V.M. Buldakov, Effect of the initial degree of spatial coherence of a light beam on intensity fluctuations in a turbulent atmosphere, *Opt. Spectrosc.* 55 (1983) 707–712.
- [5] J.C. Ricklin, F.M. Davidson, Atmospheric turbulence effects on a partially coherent Gaussian beam: implications for free-space laser communication, *J. Opt. Soc. Amer. A* 19 (2002) 1794–1802.
- [6] J.H. Churnside, Aperture averaging of optical scintillations in the turbulent atmosphere, *Appl. Opt.* 30 (1991) 1982–1994.
- [7] S. Rosenberg, M.C. Teich, Photocounting array receivers for optical communication through the lognormal atmospheric channel 2: optimum and suboptimum receiver performance for binary signaling, *Appl. Opt.* 12 (1973) 2625–2634.
- [8] E.J. Lee, V.W.S. Chan, Part 1: optical communication over the clear turbulent atmospheric channel using diversity, *IEEE J. Sel. Areas Commun.* 22 (2004) 1896–1906.

- [9] G.P. Berman, A.R. Bishop, B.M. Chernobrod, D.C. Nguyen, V.N. Gorshkov, Suppression of intensity fluctuations in free space high-speed optical communication based on spectral encoding of a partially coherent beam, *Opt. Commun.* 280 (2007) 264–270.
- [10] G.P. Berman, A.A. Chumak, Influence of phase-diffuser dynamics on scintillations of laser radiation in Earth's atmosphere: long-distance propagation, *Phys. Rev. A* 79 (2009) 063848–063854.
- [11] O. Korotkova, Scintillation index of a stochastic electromagnetic beam propagating in random media, *Opt. Commun.* 281 (2008) 2342–2348.
- [12] Y. Gu, O. Korotkova, G. Gbur, Scintillation of nonuniformly polarized beams in atmospheric turbulence, *Opt. Lett.* 34 (2009) 2261–2263.
- [13] X. Xiao, D. Voelz, Wave optics simulation of partially coherent and partially polarized beam propagation in turbulence, in: *Proc. SPIE 7464, Free-Space Laser Communications IX*, 74640T, San Diego, CA, Aug 21, 2009.
- [14] S. Avramov-Zamurovic, C. Nelson, R. Malek-Madani, O. Korotkova, Polarization-induced reduction in scintillation of optical beams propagating in simulated turbulent atmospheric channels, *Waves Random Complex Media* 24 (4) (2014) 452–462.
- [15] H. Lajunen, T. Saastamoinen, Propagation characteristics of partially coherent beams with spatially varying correlations, *Opt. Lett.* 36 (2011) 4104–4106.
- [16] Y. Gu, G. Gbur, Scintillation of nonuniformly correlated beams in atmospheric turbulence, *Opt. Lett.* 38 (2013) 1395–1397.
- [17] Y. Cai, Y. Chen, F. Wang, Generation and propagation of partially coherent beams with nonconventional correlation functions: a review [invited], *J. Opt. Soc. Amer. A* 31 (2014) 2083–2096.
- [18] L. Allen, M.W. Beijersbergen, R.J.C. Spreeuw, J.P. Woerdman, Orbital angular momentum of light and the transformation of Laguerre–Gaussian laser modes, *Phys. Rev. A* 45 (1992) 8185–8189.
- [19] J. Wang, J.Y. Yang, I.M. Fazal, N. Ahmed, Y. Yan, H. Huang, Y. Ren, Y. Yue, S. Dolinar, M. Tur, A.E. Willner, Terabit free-space data transmission employing orbital angular momentum multiplexing, *Nature Photon.* 6 (2012) 488.
- [20] M. Mirhosseini, O.S. Magana-Loaiza, M.N. O'Sullivan, B. Rodenburg, M. Malik, M.P. Lavery, R.W. Boyd, High-dimensional quantum cryptography with twisted light, *New J. Phys.* 17 (2015) 033033.
- [21] Google earth view of naval academy grounds, 2019, <https://www.google.com/maps/@38.9839544-76.4715848,963m/data=!3m1!1e3>.
- [22] A.M. Yao, M.J. Padgett, *Orbital Angular Momentum: Origins, Behavior and Applications*, OSA, Glasgow, Scotland, 2012.
- [23] Z. Chen, C. Li, P. Ding, J. Pu, D. Zhao, Experimental investigation on the scintillation index of vortex beams propagating in simulated atmospheric turbulence, *Appl. Phys. B* (2011).